Mechanisms Leading to Net Drag Reduction in Manipulated Turbulent Boundary Layers

Y. G. Guezennec*
Ohio State University, Columbus, Ohio
and
H. M. Nagib†
Illinois Institute of Technology, Chicago, Illinois

Turbulent boundary layers have been manipulated successfully using passive devices called BLADES (boundary-layer alteration devices) leading to net drag reduction. Measurements of various turbulence quantities including intermittency have led to the identification of some of the mechanisms involved in skin-friction reduction. Velocity and vorticity fluctuations associated with oncoming large scales are inhibited significantly by the manipulator blades and the vorticity shed in their wake. The manipulated boundary layers exhibit a reduced intermittency in the outer part of the layer. The effects of manipulation relax with downstream distance and the boundary layer returns toward normal conditions after 100 or 150 boundary-layer thicknesses.

Nomenclature

C_f = skin-friction coefficient
h = height of manipulator
l = chord length of manipulator
q = fluctuating component of quantity Q
q' = rms value of quantity Q
$\bar{Q}$ = long-time averaged quantity Q
$<Q>$ = short-time averaged quantity Q
Re_θ = Reynolds number, $=U_\infty\theta/\nu$
s = streamwise spacing between manipulators
t = manipulator thickness
u_τ = friction velocity
U = streamwise component of velocity
U_∞ = freestream velocity
V = normal component of velocity
x = streamwise coordinate
x_m = downstream location of first manipulator
y = normal coordinate
z = spanwise coordinate
α = flow angle, $=\tan^{-1}(V/U)$
Γ_u = intermittency based on streamwise velocity fluctuations
Γ_ω = intermittency based on spanwise vorticity fluctuations
δ = boundary-layer thickness (99.5% of U_∞)
δ^* = displacement thickness
θ = momentum thickness
ν = kinematic viscosity
ξ = nondimensional distance downstream of manipulators, $=(x-x_m)/\delta_m$
Ω_z = spanwise vorticity

Introduction

In the past decade, a growing energy consciousness has motivated a substantial amount of work aimed at viscous drag reduction. Various schemes have been proposed to alter the characteristics of the turbulent boundary layers in order to decrease the skin friction, such as addition of polymers, alterations of the wall boundary condition by various surface geometries, and modification of the turbulent structure of the boundary layer by flow manipulators. A comprehensive review of the various techniques employed as well as potential applications is given by Bushnell.[1] Among the various approaches investigated, the parallel plate manipulators, also referred to as large-eddy breakup devices (LEBUs), have been one of the most promising. A more appropriate terminology for those devices is introduced here with the acronym BLADES (boundary-layer alteration devices). Corke et al.[2,3] have shown that a carefully designed pair of two-dimensional flat plates placed in a tandem configuration within the boundary layer can yield local skin-friction reduction of up to 35% and net drag reduction of up to 20%. Comparable devices have been investigated with various degrees of success by Hefner et al.,[4,5] Bertelrud et al.,[6] Nguyen et al.,[7] Walsh and Lindemann,[8] and others. Most authors report comparable local skin-friction reduction, but the amounts of net drag reduction achieved differ widely. More recent work at the Illinois Institute of Technology by Plesniak and Nagib[9] has extended the domain of validity of Corke's results[3] and showed that the effect of the manipulators persists for at least 150 boundary-layer thicknesses downstream. They found that the key to net drag reduction resides in using high-quality manipulators associated with a low device drag.

Flow visualization[2] suggests that one of the key effects of the manipulators is the suppression of the large scales. Bradshaw[10] hypothesized that the strength of the large-scale motions is related directly to the shear stress of the wall. Hence, it is reasonable to expect that the alteration or suppression of the large scales will have a direct impact on the shear at the wall. It is also of paramount interest to investigate the downstream evolution of those "manipulated" boundary layers and examine the possible relaxation of the manipulation and return toward "regular" conditions. Various mechanisms have been proposed[3] for the suppression of the large scales, such as inhibition of the vertical velocity component of the large eddies by the manipulator blades. Other possible mechanisms for the skin-friction reduction involve the interaction of the shed vorticity in the wake of the blades with the turbulent eddies, the redistribution of the turbulent kinetic energy away from the wall, and the introduction of energetic new scales. Theoretical models have been proposed[11,12] to explain some of the effects of the manipulators on the oncoming vorticity. Although these analyses are purely inviscid, the models confirm the importance of shed vorticity in the wake of the blades as a possible vortex unwinding mechanism to reduce turbulent fluctuations in the wall region. The predicted effects of the device

Presented at the AIAA Shear Flow Control Conference, Boulder, CO, March 1985; received Sept. 8, 1987; revision received Aug. 15, 1988.

*Assistant Professor.
†Professor and Chairman. Member AIAA.

configuration seem to correlate with the parametric optimization of Plesniak and Nagib.[9]

Some of the mechanisms already have been supported by measurements or visualization, but more detailed measurements of various unsteady quantities in the manipulated boundary layers, especially in the immediate vicinity of the blades, are necessary to identify and possibly quantify the various mechanisms involved in the drag reduction process. Since both the visualization and the theoretical models point to the suppression of large scales as a plausible mode of action, it was felt that the measurement of the intermittency distribution in the manipulated boundary layer would yield a good statistical measure of the suppression of the large scales. Numerous schemes have been proposed for the determination of the intermittency function based on single or multiple components of the velocity or vorticity fluctuations. A good review of such methods is given by Hedley and Keffer.[13] Since the passage of large scales should be associated with substantial spanwise vorticity fluctuations, the determination of the particular vorticity component was deemed important for evaluating the intermittency function. In addition, the documentation of other unsteady quantities such as streamwise and normal velocity fluctuations and Reynolds stresses especially in the near vicinity of the blades should help identify some of the mechanisms outlined above and possibly lead to a better design of the manipulators in terms of net drag reduction.

Experimental Procedure

The experiment was performed in the high-speed test section of the M. V. Morkovin wind tunnel. The tunnel is operated in a closed return mode and has a turbulence intensity of 0.1% for velocities ranging up to 35 m/s. The 5.1-m-long test section has a rectangular cross section 0.6 m wide and 0.9 m high. The turbulent boundary layers were developed over a smooth flat plate suspended in the test section at one-third of its height. The leading edge of the plate was machined to a very sharp edge slightly curved downward. A low-solidity perforated plate was placed at the downstream end of the test section on the upper side of the flat plate, hence creating a slight pressure difference between the two sides of the plate. This insured that the stagnation streamline impinged on the measurement side of the plate. A strip of No. 24. grit sandpaper was placed 10 cm downstream of the leading edge to fix the transition at that location rather than to trip the boundary layer. The freestream velocity used throughout the experiment was nominally 18 m/s, with a slightly adverse pressure gradient in the last 180 cm of the test section. All measurements were preformed on the centerline of the plate at six stations, A-F. A schematic diagram of the test plate showing the position of the measurement stations and of the manipulators is illustrated in Fig. 1. A computer-controlled traversing mechanism placed on the top of the tunnel supported the various probes used in this investigation.

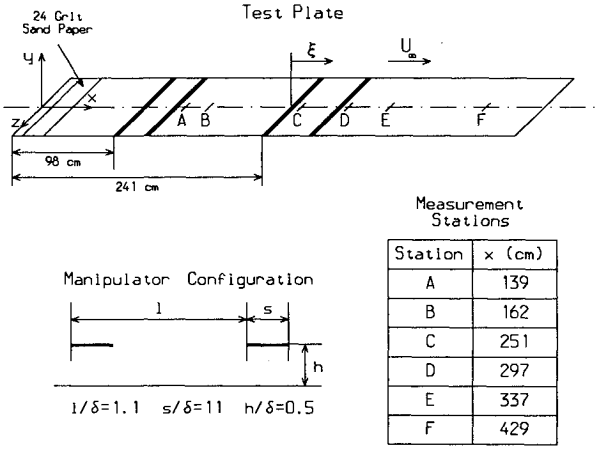

Station	x (cm)
A	139
B	162
C	251
D	297
E	337
F	429

Fig. 1 Schematic diagram of boundary-layer test plate and manipulator configuration.

Three flow conditions were investigated:

1) A "regular" case corresponding to a naturally developing turbulent boundary layer, with Reynolds numbers based on momentum thickness ranging between 3 and 8.8×10^3.

2) A "downstream manipulated" case corresponding to the same boundary layer in which a pair of tandem flat-plate manipulators was placed at $x_m=241$ cm. The configuration of the manipulator was chosen according to the findings of Plesniak and Nagib[9] to yield optimal drag reduction. The geometrical configuration of the manipulators is also shown in Fig. 1. This positioning of the manipulators allowed the evolution of the manipulated boundary layer to be followed over 50 boundary-layer thicknesses. Most of the measurements reported in this paper were obtained with this configuration.

3) An "upstream manipulated" case for which the manipulators were placed at $x_m=98$ cm. This case was primarily designed to study the evolution of the manipulated boundary layers at large distances downstream of the devices (up to 140 boundary-layer thicknesses) to assess the possible relaxation of the boundary layer and return toward "regular" conditions.

Each case was first documented using a single hot-wire probe to determine the mean characteristics of the boundary layers. A series of profiles was taken on the centerline of the plate at various downstream distances. A two-dimensional momentum balanced technique[3] was used to compute the local skin friction and the overall drag on the plate. The turbulent characteristics of the boundary layers were then determined from a set of profiles taken with a four-wire transverse vorticity probe similar to the one used by Foss.[14] The probe consists of an X array and a parallel array side by side. Special attention was given to the design of the probe to minimize the prong interference and the spatial extent of the probe.

All of the hot-wire signals, as well as the air temperature, freestream velocity, and probe position were acquired digitally and stored on magnetic tape for later processing. The sampling rate was such that the time resolution was commensurate with the spatial resolution of the probe (approximately 50-70 wall units). The record length was on the order of 100 outer scales, and 50 records were acquired at each spatial location to insure good statistical convergence. The hot-wire signals were temperature compensated and calibrated using squared third-order polynomials (see Ref. 3 for more details). The X array of the vorticity probe was used to determine the streamwise and normal velocity components. The parallel array yielded the normal gradient of the streamwise velocity for the computation of the spanwise vorticity. The second term in the vorticity expression was estimated using Taylor's hypothesis from the time derivative of the normal component divided by the convection velocity over the probe, i.e.,

$$\Omega_z=\frac{\partial V}{\partial x}-\frac{\partial U}{\partial y}\approx\frac{1}{U_\infty}\frac{\partial V}{\partial t}-\frac{\partial U}{\partial y}$$

The intermittency function was computed based on $<(\partial U/\partial t)^2>$, $<u'v'>$, and $<\omega_z'^2>$ (see Ref. 13 for a review of the various techniques). All methods involved sensitizing the signal, averaging over a short interval, and thresholding. Hence, a certain degree of arbitrariness is inherent to the determination of the intermittency function. To alleviate this problem, a systematic investigation of the two parameters (threshold and hold time) was performed for all three schemes utilizing data taken in the *regular boundary layer*. With an "appropriate" choice of the threshold and hold time, the methods were found to be in good agreement. Arbitrarily, the "appropriate" values of the parameters were defined as those values yielding an intermittency distribution

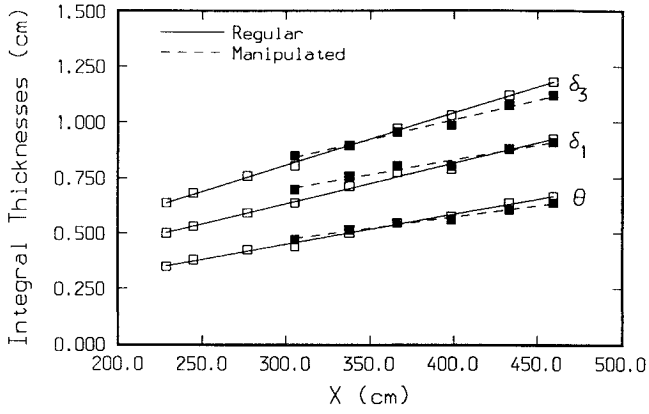

Fig. 2 Comparison of integral thicknesses for regular and downstream manipulated boundary layers.

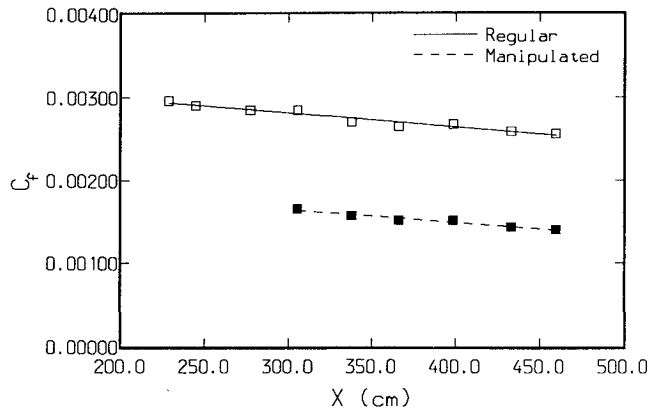

Fig. 3 Comparison of skin-friction coefficient for regular and downstream manipulated boundary layers.

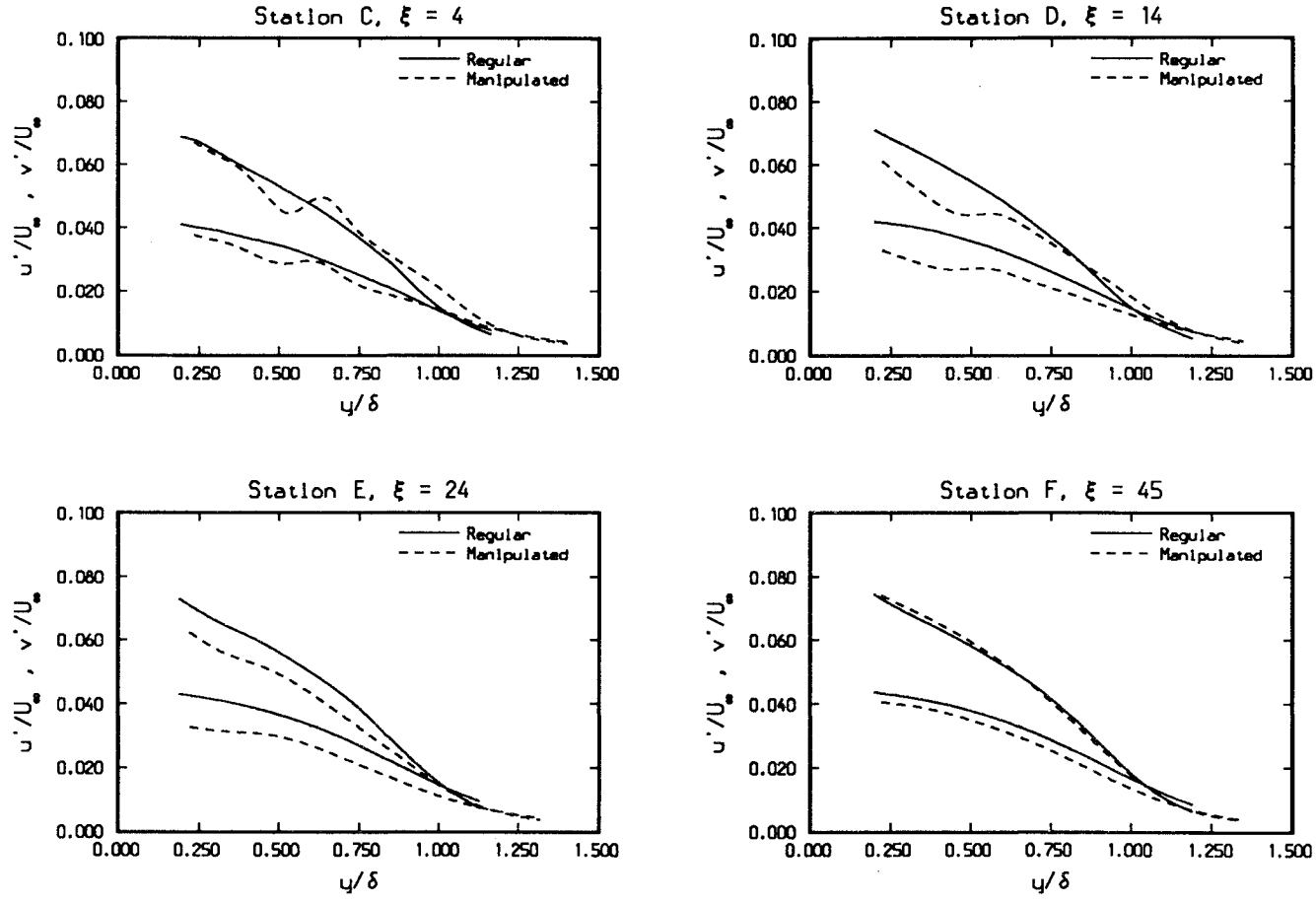

Fig. 4 Comparison of streamwise and normal turbulence intensity profiles for regular and downstream manipulated boundary layers.

and associated time scales comparable to those reported by other investigators[13] in zero-pressure-gradient boundary layers. This choice was deemed to be reasonable since the pressure gradient in our "regular" boundary layer was extremely mild. Once chosen for a particular method in the regular boundary layer, those values were kept constant (after nondimensionalization by the appropriate outer variables) for all of the cases investigated.

Results

Figure 2 illustrates the global effect of the manipulators on the mean characteristics of the boundary layer. The various integral thicknesses are plotted vs downstream distance for both the regular and downstream manipulated cases. The manipulated case exhibits an initially higher momentum thickness indicative of the device drag. However, the rate of growth of the momentum thickness, θ, is substantially reduced and leads to a reduction in the local skin friction. The displacement thickness, δ^*, follows a similar trend. A momentum balance technique was then used to correct for the very mild pressure gradient and to compute the skin friction, C_f. The implementation and validation of the momentum balance technique used here can be found in Refs. 2 and 9. In particular, the issue of three-dimensional effects was addressed in Ref. 9, and

spanwise measurements of the various integral quantities were performed. Skin-friction estimates based on such spanwise measurements did not differ substantially from two-dimensional centerline estimates. Figure 3 shows that a local skin-friction reduction on the order of 40% is achieved and persists for at least 45 boundary-layer thicknesses. The magnitude of the initial skin-friction reduction is commensurate with that observed by other investigators. The apparent lack of relaxation of the skin friction with downstream distance may be an artifact of the momentum balance technique performed over a limited downstream distance. Similar measurements performed in the upstream manipulated case (see Ref. 15) do show a slow relaxation of the skin friction over larger downstream distances.

The streamwise and normal turbulence intensity profiles are shown in Fig. 4. These profiles are nondimensionalized by the local boundary-layer thickness δ (height at which the velocity reaches 99.5% of its freestream value). The manipulators first reduce the normal velocity fluctuations immediately downstream of the first manipulator (station C). After the second manipulator (station D), the normal component is further suppressed and, subsequently, the streamwise component is also attenuated, especially below the wake of the manipulators. The presence of energetic scales in the wake of the blades clearly is identifiable in both components of the turbulence intensity. By station E, the turbulence in the wake is no longer distinguishable from the background turbulence. However, both components are less energetic than their counterparts in the regular boundary layer. By station F ($\xi = 45$), the streamwise component has relaxed to a normal level, but the normal component still remains attenuated. This attenuation of the normal component is in good agreement with the theoretical models referred to earlier.

Figure 5 shows the downstream evolution of the profiles for the mean flow angle α. The mean flow angle is positive, reflecting the growth of the boundary layer. The regular boundary layer is characterized by a fairly constant angle throughout the boundary layer, with slightly higher values in the inner part. The manipulated boundary layer exhibits substantially higher mean angles in the lower part. This could be interpreted as a thickening of the wall layer, which is consistent with the reduction in skin friction. This effect progressively relaxes with downstream distance. Additional measurements were performed in the immediate vicinity of the second manipulator at 1.25, 2.5, and 5.0 cm downstream of the trailing edge, respectively. A mild downwash is observed in the wake. This downwash was conjectured by Plesniak and Nagib[9] and is believed to play a key role in obtaining net drag reduction by providing a displacement control of the mean flow in the boundary layer.

The Reynolds stress profiles are shown in Fig. 6 in nondimensionalized form. In the initial region downstream of the devices, the Reynolds stress profiles exhibit a drastic reduction below the wake of the manipulator. This large Reynolds stress deficit persists as long as the wake is associated with energetic scales. As the wake decays with downstream distance, the Reynolds stress deficit is redistributed throughout the boundary layer and gradually relaxes back to the normal values. This evolution of the Reynolds stress in the manipulated boundary layer illustrates the important role played by the wake in the

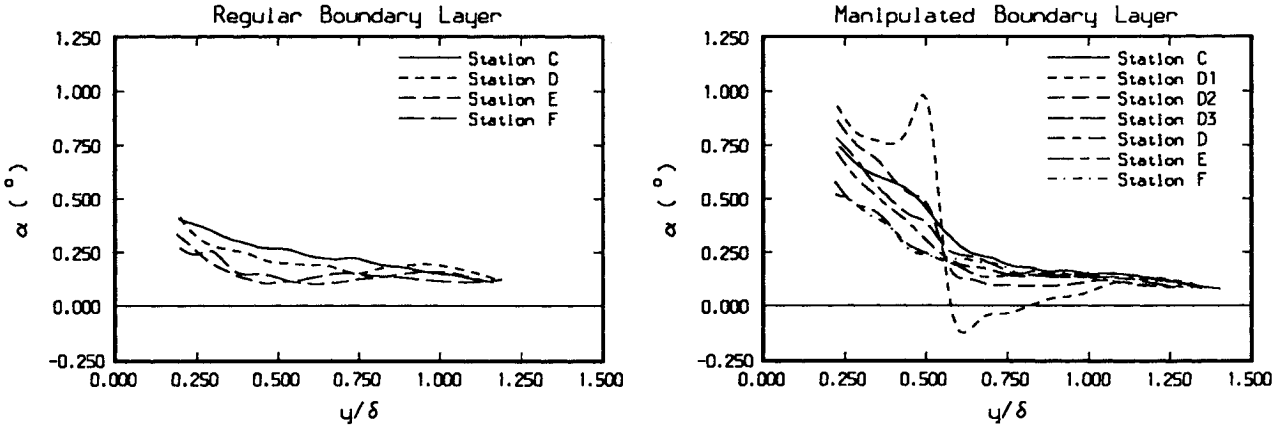

Fig. 5 Downstream evolution of mean flow angle profiles for regular and downstream manipulated boundary layers.

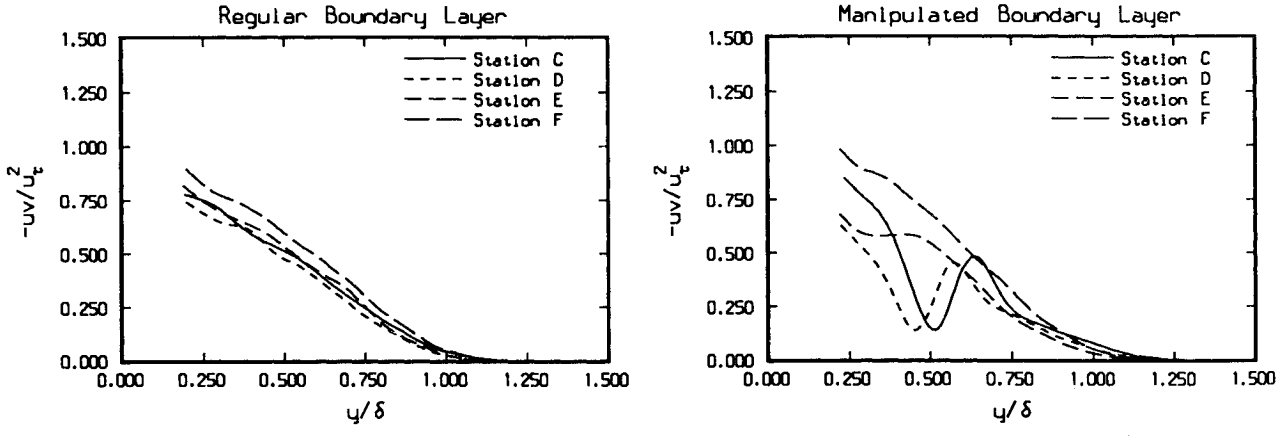

Fig. 6 Downstream evolution of Reynolds stress profiles for regular and downstream manipulated boundary layers.

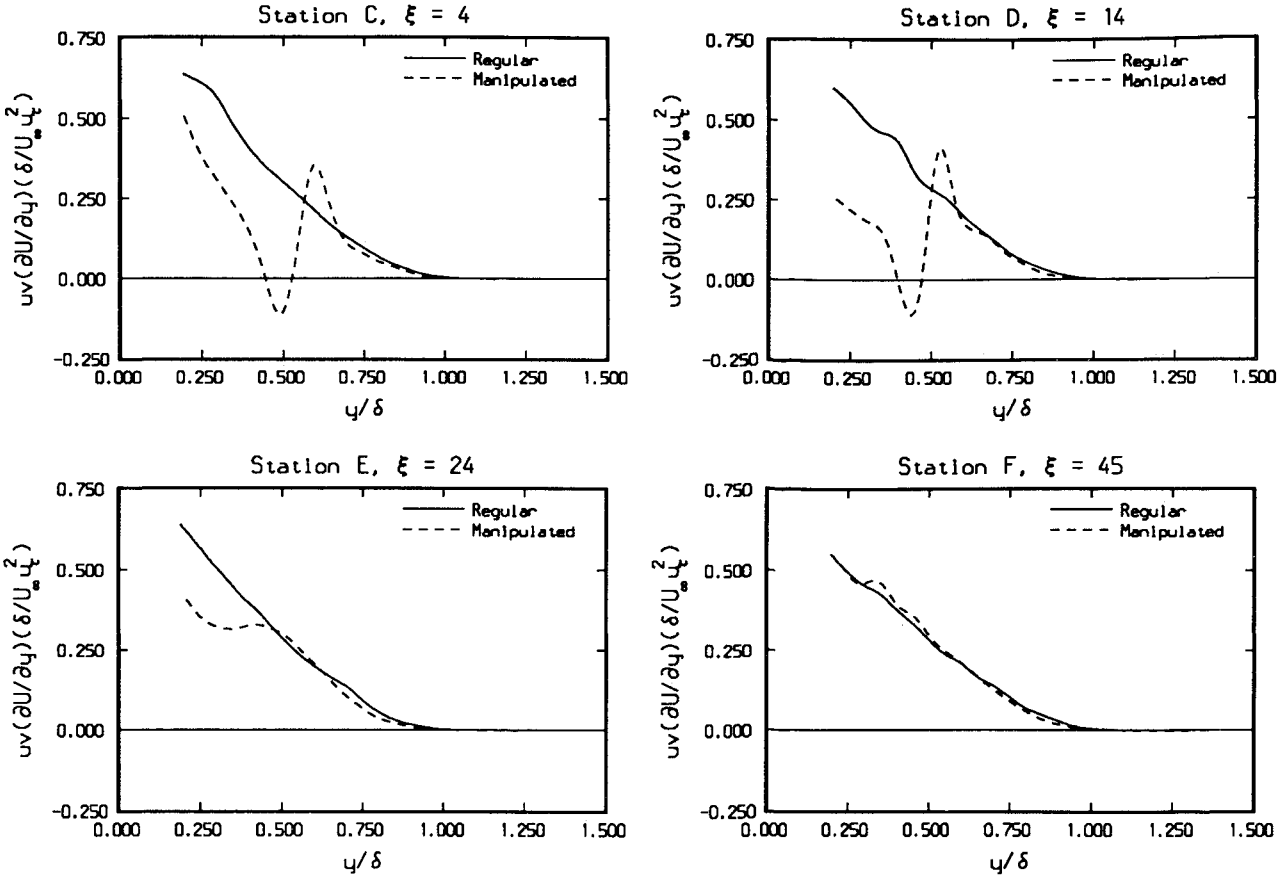

Fig. 7 Comparison of turbulence production profiles for regular and downstream manipulated boundary layers.

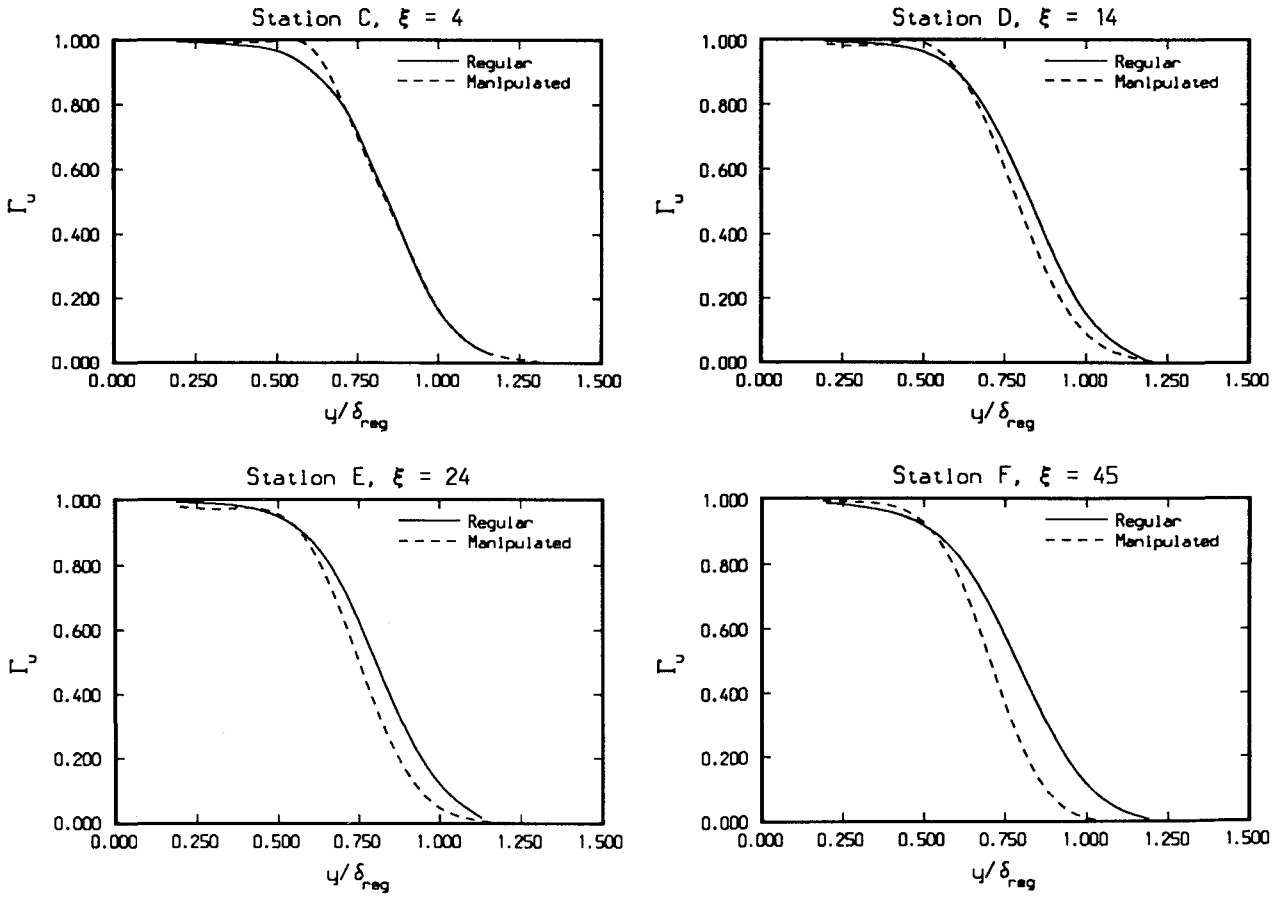

Fig. 8 Comparison of intermittency profiles based on streamwise velocity fluctuations for regular and downstream manipulated boundary layers.

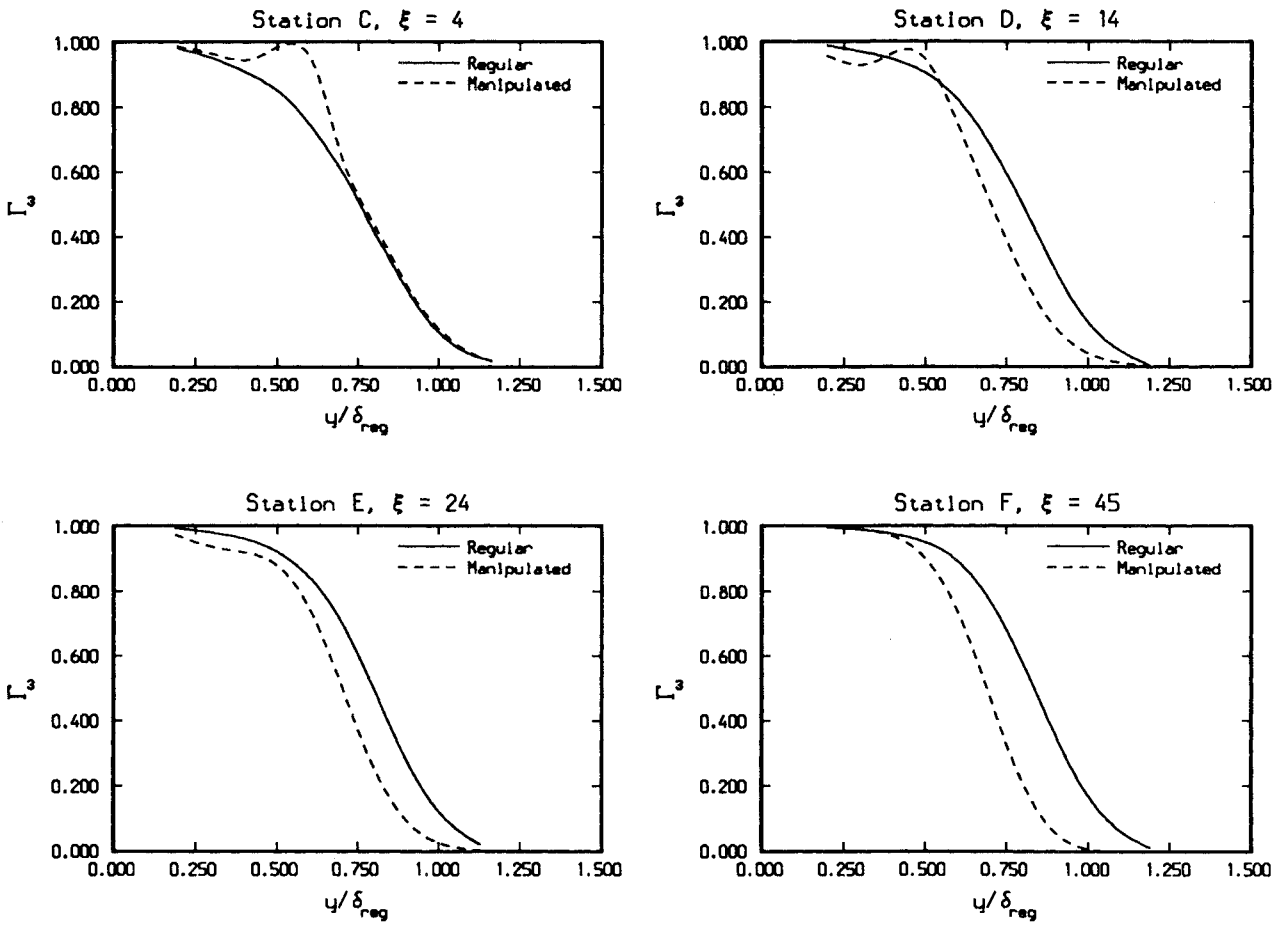

Fig. 9 Comparison of intermittency profiles based on spanwise vorticity fluctuations for regular and downstream manipulated boundary layers.

suppression of the large scales, through either an interaction of the shed vorticity with the large eddies (vortex unwinding) or the redistribution of the turbulent kinetic energy by the wake (turbulence pumping). This effect can be identified more clearly by considering an estimate of the turbulence production as shown in Fig. 7. A large pocket of near-zero production is detected under the wake, while an excess production develops above the wake. This effect redistributes some of the turbulent kinetic energy away from the wall. The small region of negative production can be attributed to the fact that the sign reversals of the Reynolds stress and the mean shear do not coincide exactly.

Figure 8 shows the comparison of the intermittency distribution between the regular and manipulated boundary layers at four measuring stations. The intermittency was evaluated here from the streamwise velocity fluctuations (Γ_u). The local thickness of the regular boundary layer was used to nondimensionalize the vertical coordinate. At station C, immediately downstream of the first manipulator, the intermittency profile is not affected appreciably except for the locally higher turbulence in the wake of the blade. The suppression of the large scales becomes evident after the second manipulator. The reduced intermittency spans the whole boundary-layer thickness, indicating that the scales affected by the manipulation process are of the order of the boundary thickness, i.e., the large eddies. This effect clearly persists up to station F, 45 boundary-layer thicknesses downstream of the manipulators. The manipulated case is characterized by a steepening of the intermittency profiles or, in other words, a less corrugated interface between turbulent and nonturbulent fluids. This confirms the results of former visualization studies. The thinning of the manipulated boundary layer with respect to the regular case is also evident.

A similar comparison between the two boundary layers is shown in Fig. 9 for the intermittency based on the spanwise vorticity fluctuations (Γ_ω). The various effects are even more clearly identifiable, i.e., a substantial reduction of the intermittency in the outer part of the boundary layer and below the wake, taking place immediately downstream of the manipulators. The persistence of an organized wake for at least 25 boundary-layer thicknesses underlines the importance of the shed vorticity in the manipulation process.

Figure 10 shows the comparison of turbulent, T_t, and potential, T_p, time scales associated with the intermittency (average period of time during which the flow is turbulent or nonturbulent, respectively). The time scales have been nondimensionalized by outer scales, namely, the boundary-layer thickness and the freestream velocity. Figure 10 also shows that the reduced intermittency in the manipulated case corresponds mainly to a reduction of the turbulent time in the inner part of the boundary layer and to an increase of the potential time in the outer part.

The relaxation of the manipulated boundary layer toward equilibrium is addressed in Fig. 11. This figure shows a comparison of the downstream evolution of the intermittency distribution, Γ_u, between the regular boundary layer and the upstream manipulated boundary layer. In the regular case, the intermittency profiles remain self-similiar in shape as the Reynolds number, Re_θ, is increased from $3\text{–}8.8\times10^3$. However, the profiles monotonically shift toward the left. This evolution is consistent with the concept of "aging" of boundary layers[3] also documented visually, by which large-sale motions near the outer edge of the boundary layer are engulfed slowly by wall turbulence. On the other hand, the manipulation results in an immediate steepening of the intermittency profile after the manipulators. Then, two effects take place with

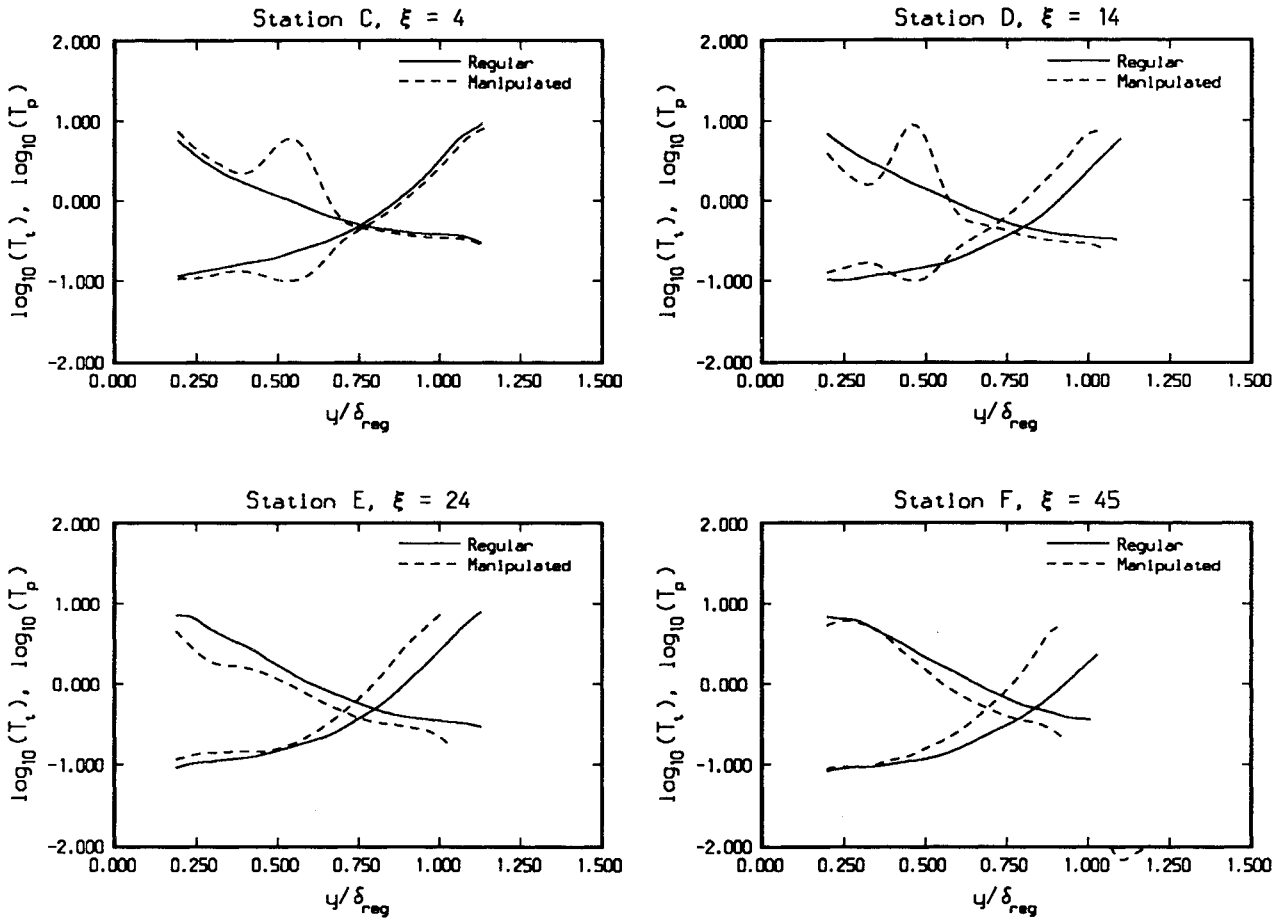

Fig. 10 Comparison of turbulent and potential time-scale profiles for regular and downstream manipulated boundary layers.

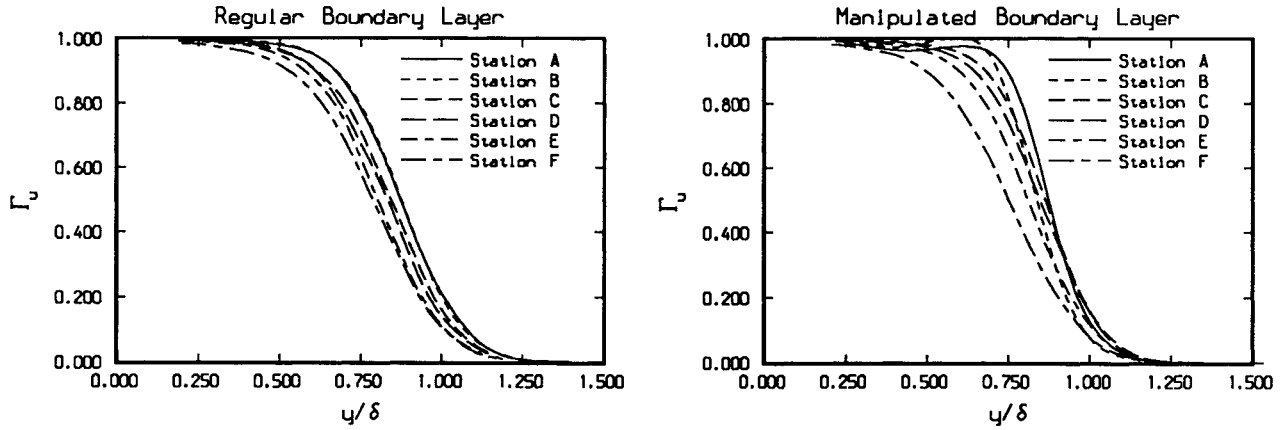

Fig. 11 Downstream evolution of intermittency profiles based on streamwise velocity fluctuations for regular and upstream manipulated boundary layers.

downstream distance: a gradual shift to the left indicative of the normal aging of the boundary layer and a slow relaxation of the slope of intermittency profiles toward regular conditions at the last measuring station, 140 boundary-layer thicknesses downstream of the manipulators.

Conclusions

In summary, the various mechanisms proposed earlier have been confirmed and documented in detail, namely:

1) An immediate effect resulting from the inhibition of the normal velocity component of the large scales by the manipulators, as illustrated by the intermittency and normal turbulence intensity profiles. The evidence of the suppression of large scales is supported by the marked difference in the intermittency profiles based on the transverse vorticity fluctuations.

2) A persisting suppression due to the vorticity shed in the wake of the manipulators that interacts with the oncoming vorticity to reduce the normal velocity fluctuations near the wall. This effect is in good agreement with the vortex unwinding models mentioned earlier.

3) A redistribution of the turbulent kinetic energy by the wake of the manipulators. This results in a lower turbulence production in the wall region below the wake.

4) A mild downwash generated by the circulation field around the manipulators that contributes to the displacement control of the mean flow and the thinning of the boundary layer.

5) The introduction of new energetic smaller scales in the wake of the manipulators that interact with the existing scales in the boundary layer and affect the global energy production and transfer between the wall region and the rest of the layer.

The mechanisms identified here provide an explanation for the height optimization results of Plesniak and Nagib.[9] The inhibition of turbulent velocity fluctuations and production takes place underneath the wake of the manipulators. Hence, by placing the manipulators lower in the boundary layer the wall region is affected more directly. The skin friction decreases accordingly as a result of the relative quiescence in that region.

In addition, the effect of the BLADES at large downstream distances has been investigated. The direct and induced effects of the manipulators on the streamwise turbulence intensity and Reynolds stress profiles seem to relax after 50 boundary-layer thicknesses. However, the attenuation of the normal component persists longer. The intermittency profiles slowly return to normal conditions after 150 boundary-layer thicknesses. These trends are consistent with the findings of Plesniak and Nagib[9] indicating that the largest part of the net drag reduction occurs over the first 50 boundary-layer thicknesses, althought the skin friction relaxes to normal at approximately 150 boundary-layer thicknesses.

In summary, three regions of action of the BLADES have been identified:

1) A local or "immediate" effects region corresponding to the location of the manipulators, where the effects are governed mainly by the change in boundary conditions imposed on the flow (i.e., direct suppression).

2) A near or "persistent" effects region spanning the first 20–40 boundary-layer thicknesses downstream of the manipulators, where the effects stem from a balance between the relaxation of the immediate effects and contributions of new flow alteration modules (e.g., shed vorticity in the wake, new scales).

3) A far or "relaxation" region ranging up to 100–150 boundary-layer thicknesses, where the aforementioned mechanisms are not active and the boundary layer gradually returns to an equilibrium state.

Based on the preceding understanding, remanipulation of the boundary layer as early as 50 boundary-layer thicknesses downstream of the first BLADE is feasible although probably not optimal. This concept was verified successfully by Plesniak[15] and led to an additional 10% net drag reduction.

Acknowledgments

The authors would like to acknowledge the support of this research by the NASA Langley Research Center and the Air Force Office of Scientific Research under Grant NSG-1591.

References

[1]Bushnell, D. M., "Turbulent Drag Reduction for External Flows," AIAA Paper 83-0227, Jan. 1983.

[2]Corke, T. C., Guezennec, Y. G., and Nagib, H. M., "Modification in Drag of Turbulent Boundary Layers Resulting from Manipulation of Large-Scale Structures," NASA CR-3444, July 1981.

[3]Corke, T. C., Nagib, H. M., and Guezennec, Y. G., "A New View on Origin, Role and Manipulation of Large Scales in Turbulent Boundary Layers," NASA CR-165861, Feb. 1982.

[4]Hefner, J. N., Weinstein, L. M., and Bushnell, D. M., "Large-Eddy Breakup Scheme for Turbulent Viscous Drag Reduction," *Progress in Aeronautics and Astronautics: Viscous Flow Drag Reduction,* edited by G. R. Hough, AIAA, New York, Vol. 72, 1980, pp. 110–127.

[5]Hefner, J. N., Anders, J. B., and Bushnell, D. M., "Alteration of Outer Flow Structures for Turbulent Drag Reduction," AIAA Paper 83-0293, Jan. 1983.

[6]Bertelrud, A., Truong, T. V., and Avellan, F., "Drag Reduction in Boundary Layers Using Ribbons," AIAA Paper 82-1370, Aug. 1982.

[7]Nguyen, V. D. et al., "Some Experimental Observations of the Law of the Wall Behind Large-Eddy Breakup Devices Using Servo-Controlled Skin Friction Balances," AIAA Paper 84-0346, Jan. 1984.

[8]Walsh, M. J. and Lindemann, A. M., "Optimization and Application of Riblets for Turbulent Drag Reduction," AIAA Paper 84-0347, Jan. 1984.

[9]Plesniak, M. and Nagib, H. M., "Net Drag Reduction in Turbulent Boundary Layers Resulting from Optimized Manipulation," AIAA Paper 85-0518, March 1985.

[10]Bradshaw, P., "The Turbulent Structure of Equilibrium Boundary Layers," *Journal of Fluid Mechanics,* Vol. 29, Pt. 4, 1967, pp. 625–645.

[11]Dowling, A. P., "The Effect of Large Eddy Break-Up Devices on Oncoming Vorticity," University Engineering Dept., Cambridge Univ., England, Internal Rept. 1984.

[12]Balakumar, P. and Widnall, S. E., "Application of Unsteady Aerodynamics to Large-Eddy Breakup Devices in a Turbulent Flow," *Physics of Fluids,* Vol. 29, 1986, pp. 1779–1786.

[13]Hedley, T. B. and Keffer, J. F., "Turbulent/Non-Turbulent Decisions in an Intermittent Flow," *Journal of Fluid Mechanics,* Vol. 64, 1974, 625–644.

[14]Foss, J. F., "Advanced Techniques for Transverse Vorticity Measurement," *Proceedings of 7th Biennal Symposium on Turbulence,* Univ. of Missouri-Rolla, 1981, pp. 29-1–29-12.

[15]Plesniak, M. W., "Optimized Manipulation of Turbulent Boundary Layers Aimed at Drag Reduction" M. Sc. Thesis, Illinois Inst. of Technology, Chicago, Dec. 1985.